doi: 10.1111/j.1365-3121.2005.00612.x

Dating faulted alluvial fans with cosmogenic ^{10}Be in the Gurvan Bogd mountain range (Gobi-Altay, Mongolia): climatic and tectonic implications

Riccardo Vassallo,[1] Jean-François Ritz,[1] Régis Braucher[2] and Sébastien Carretier[3]

[1]*Laboratoire Dynamique de la Lithosphère, UMR 5573 Université Montpellier II, Montpellier, France;* [2]*CEREGE, Europole Méditerranéen de l'Arbois, Aix-en-Provence, France;* [3]*BRGM/ARN3, Orléans, France*

ABSTRACT

The Gurvan Bogd mountain range is a fault system characterized by strong earthquakes (M ~ 8) separated by long periods of quiescence. Further to the previous works in the area, our study provides new data concerning the tectonic and climatic processes in the Gobi-Altay. To quantify the slip rates along the faults, we dated offset alluvial fans analysing the *in situ* produced ^{10}Be along profiles at depth. The slip rates along the Bogd strike–slip fault and its associated thrust faults over the Upper Pleistocene–Holocene period are 0.95 ± 0.29 mm yr^{-1} and comprised between 0.12 ± 0.02 and 0.13 ± 0.02 mm yr^{-1}, respectively. The surfaces ages account for a cyclic formation of the fans over the past ~360 ka, in correlation with the terminations of the marine isotope stages 2, 6, 8 and 10.

Terra Nova, 17, 278–285, 2005

Introduction

The seismic cycle is often much longer than the instrumental or even the historical seismicity record periods (e.g. McCalpin, 1996; Yeats and Prentice, 1996). It is particularly true in intracontinental domains, where the accumulation of strain is slow and where recurrence intervals of earthquakes can reach several thousand years. One of the means to characterize the activity of faults in such settings is to determine their long-term slip rates by dating offset morphological features. This implies the use of geochronological methods, such as the *in situ* ^{10}Be dating (e.g. Brown *et al.*, 1991; Brook *et al.*, 1993), which can be applied to periods of time as long as 10 000–500 000 years.

In this paper, we present the results of a slip-rate analysis on several segments of the Gurvan Bogd fault system in the Gobi-Altay, Mongolia (Fig. 1), where one of the largest intracontinental earthquakes (M8.3) occurred in 1957 (Florensov and Solonenko, 1965; Kurushin *et al.*, 1997). The Bogd fault, the main strike–slip

Correspondence: Jean-François Ritz, Laboratoire Dynamique de la Lithosphère, UMR 5573 Université Montpellier II, place E. Bataillon 34095 Montpellier Cedex 05, France. Tel.: +33 (0)4 67 14 39 07; fax: +33 (0)4 67 14 36 42; e-mail: ritz@dstu.univ-montp2.fr

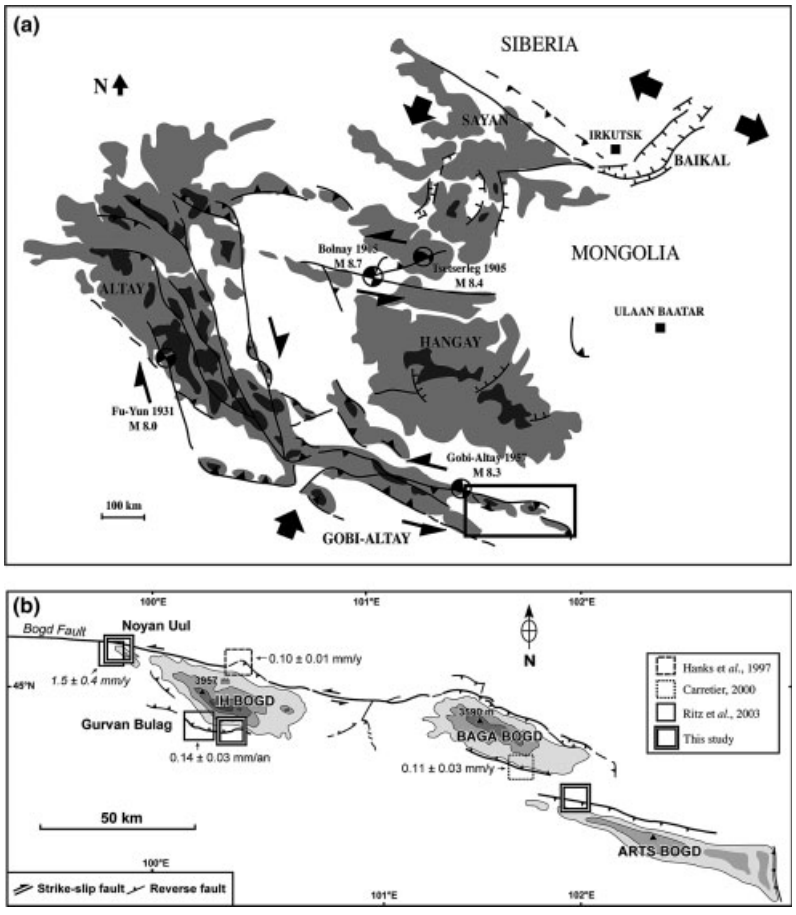

Fig. 1 (a) Simplified map of the principal mountain ranges and associated active faults in Western Mongolia. Focal mechanisms of the four M > 8 earthquakes of the twentieth century are indicated. (b) Close-up of the Gurvan Bogd range in the Gobi-Altay, with the Upper Pleistocene fault slip rates determined by previous works (vertical and horizontal components are in normal and italics characters, respectively) and the location of the studied sites.

Table 1 Results of ^{10}Be analysis at the Tandetron AMS facility, Gif-sur-Yvette, France (Raisbeck *et al.*, 1987). Measured ^{10}Be/^{9}Be ratios were calibrated directly against the National Institute of Standards an Technology (NIST) standard reference material SRM 4325 using its certified ^{10}Be/^{9}Be ratio of $(26.8 \pm 1.4) \times 10^{-12}$. Surface production rates were obtained from calculation based on the latitude–altitude-dependent polynomials of Lal (1991)

Sample	Depth (cm)	Density (g cm^{-3})	Production (at g^{-1} yr^{-1})	^{10}Be (Mat g^{-1})	Error ^{10}Be (Mat g^{-1})
NU42	205	2.70	1.01	0.34	0.06
NU45	160	2.70	1.80	0.63	0.14
NU47	110	2.70	3.82	0.45	0.07
NU49	80	2.70	6.25	0.32	0.04
NU51	20	2.70	17.53	1.11	0.16
NU52A	0	2.70	24.91	1.85	0.27
ABW1	200	2.75	0.92	0.42	0.10
ABW4	160	2.75	1.55	0.74	0.09
ABW6	120	2.75	2.83	1.23	0.14
ABW8	80	2.75	5.48	2.41	0.32
ABW10	40	2.75	10.97	3.29	0.41
ABW12B	0	2.75	22.38	3.39	0.37
IBSA23	140	2.65	2.55	0.54	0.07
IBSA25	100	2.65	4.73	0.73	0.09
IBSA26	70	2.65	7.73	1.37	0.19
IBSA28	30	2.65	15.18	1.79	0.20
IBSA30	0	2.65	25.45	2.54	0.27
IBSB31	200	2.65	1.15	0.16	0.04
IBSB33	160	2.65	1.91	0.38	0.05
IBSB35	120	2.65	3.45	0.15	0.03
IBSB37	80	2.65	6.55	0.37	0.05
IBSB39	40	2.65	12.80	0.50	0.07
IBSB41	0	2.65	25.45	0.70	0.10

fault segment, has been among the first examples studied in terms of slip-rate analysis using ^{10}Be dating (e.g. Ritz *et al.*, 1995). This study consisted in measuring *in situ* produced ^{10}Be at the surface of offset markers such as alluvial fans. Three other studies (i.e. Hanks *et al.*, 1997; Carretier, 2000; Ritz *et al.*, 2003) have been carried out in the area bringing estimates of long-term slip rates – either horizontal or vertical – along some of the main fault segments (Fig. 1b). Moreover, ^{10}Be dating has shown that alluvial fans within this region form episodically and seems correlated with the terminations of glacial stages (Ritz *et al.*, 1995, 2003).

These studies, as several others in similar context (e.g. Anderson *et al.*, 1996; Repka *et al.*, 1997; Van der Woerd *et al.*, 1998; Hancock *et al.*, 1999; Brown *et al.*, 2002), showed that superficial samples often contained inherited ^{10}Be due to pre-exposure. This inheritance adds to the ^{10}Be concentration accumulated after abandonment of the surfaces and leads to the overestimation of their exposure ages. To better constrain the dating, it appeared necessary to look at the distribution of ^{10}Be at depth

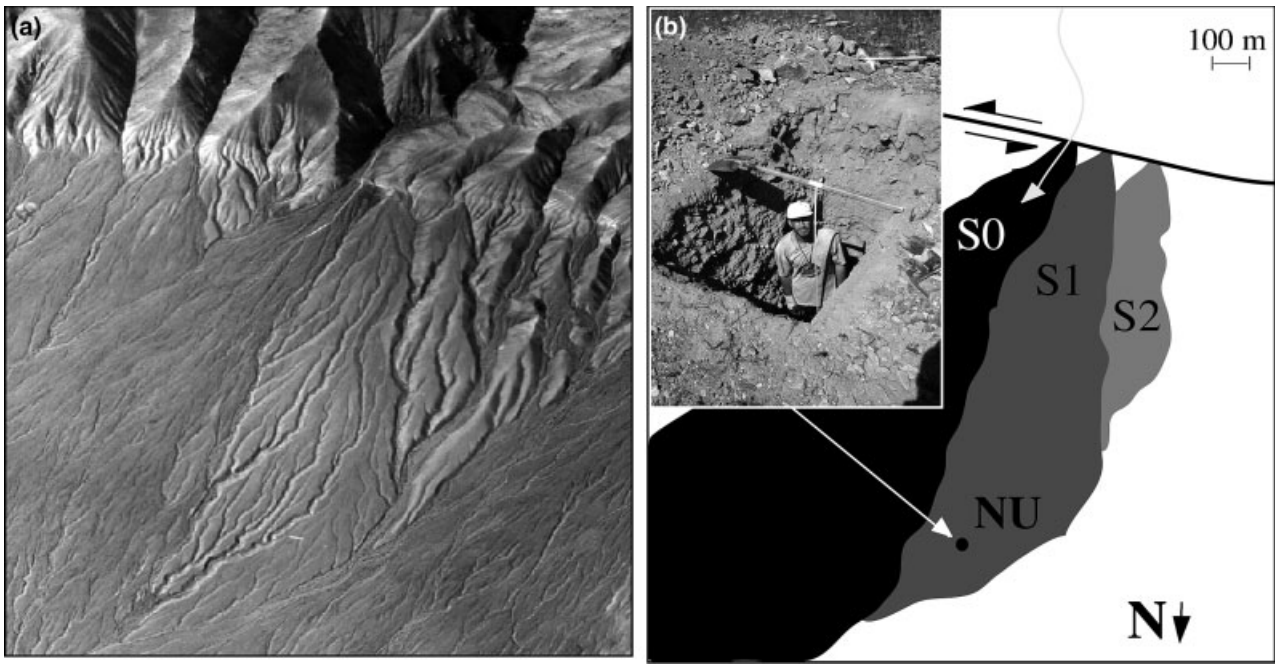

Fig. 2 (a) Aerial photograph of the studied site along the Bogd fault at Noyan Uul. (b) Corresponding morphotectonic interpretation of the offset alluvial surfaces and location of the ^{10}Be sampling site. The picture in the top-left corner shows the hand-dug soil pit for ^{10}Be sampling at depth.

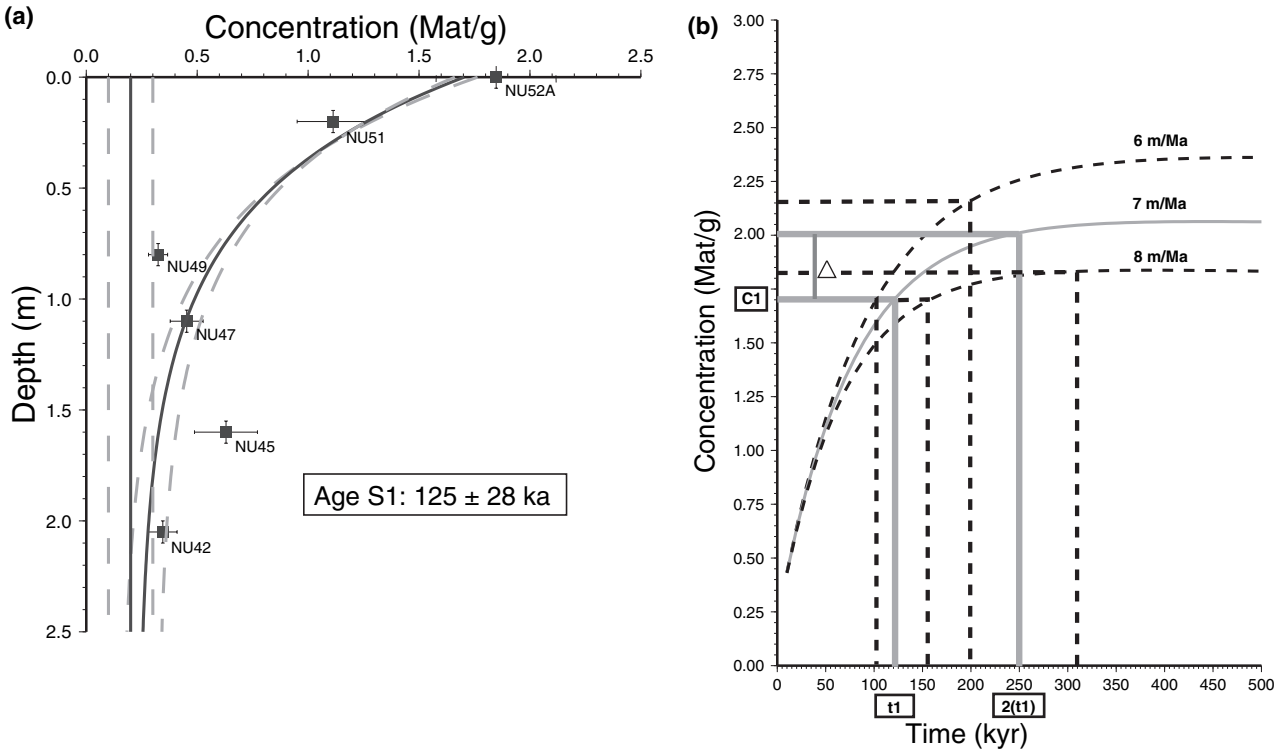

Fig. 3 (a) Results of the ^{10}Be analysis of surface S1 at Noyan Uulsite; the best-fit exponential decrease model is in solid line and models with minimum and maximum average inheritance are in dashed lines. (b) Diagram of the evolution of the surface ^{10}Be concentration vs. time showing the calculation of S1 and S2 surface ages (see text for explanation).

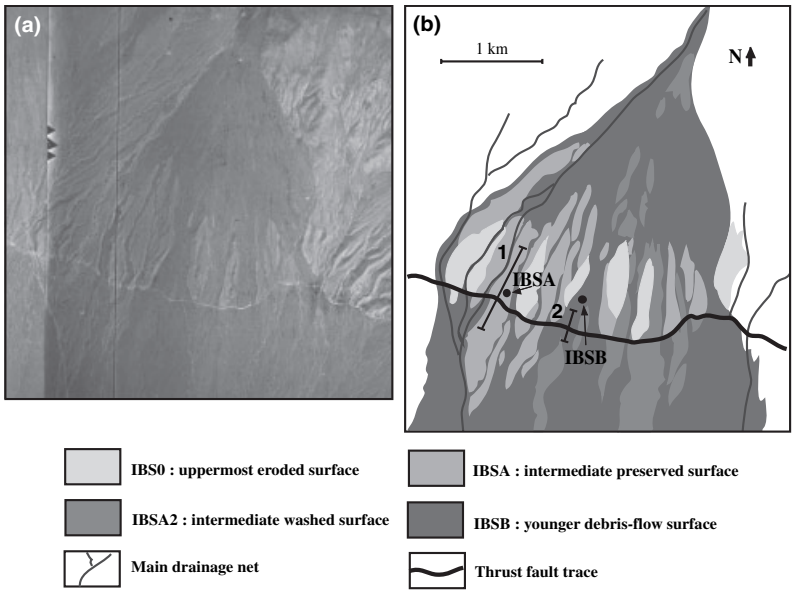

Fig. 4 (a) Aerial photograph of the studied site along the Gurvan Bulag thrust fault. (b) Corresponding detailed morphotectonic map (after Ritz *et al.*, 2003) with location of the ^{10}Be sampling sites and of the topographic profiles (see Fig. 5a).

and check its theoretically predicted exponential decrease in a vertical profile (e.g. Brown *et al.*, 1992). In this study, we used *in situ* ^{10}Be to date offset surfaces by analysing the ^{10}Be distribution at depth in order to quantify the average pre-exposure of sediments. We have re-examined the site studied by Ritz *et al.* (1995) at Noyan Uul along the Bogd fault where a 1.2 mm yr^{-1} maximum horizontal slip rate was estimated, and studied two new sites along the Gurvan Bulag fault and along the Artz Bogd fault (see Fig. 1b).

Tectonic setting

Western Mongolia is affected by a NNE–SSW compression related to the India–Asia collision (Tapponnier and Molnar, 1979) (Fig. 1a). Deformation is transpressional and characterized by large strike–slip faults associated with reverse faults surrounding the Hangay Dôme (e.g. Baljinnyam *et al.*, 1993; Cunningham *et al.*, 1996; Schlupp, 1996). To the South, in Gobi-Altay, main fault trends are N100E and correspond to left-lateral strike–slip faults, whereas to the West, in Altay, main fault trends are N140E and correspond to right-lateral strike–slip faults.

The Gurvan Bogd mountain range corresponds to the easternmost part of

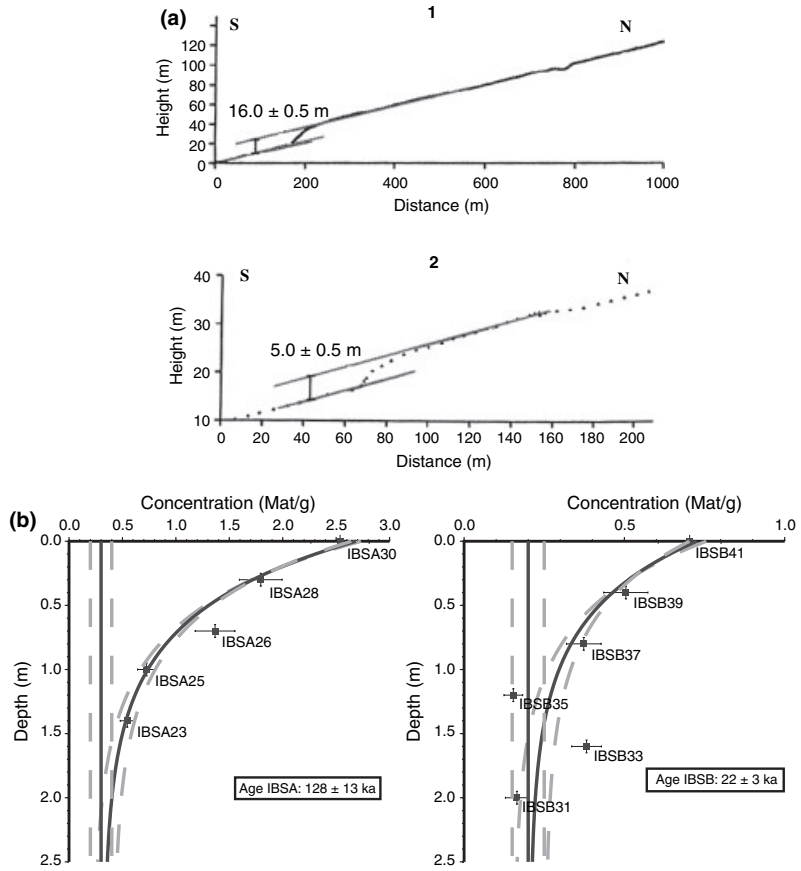

Fig. 5 (a) Topographic profiles across the two surfaces IBSA and IBSB and vertical offsets at Gurvan Bulag site. (b) Results of the ^{10}Be analysis on the two surfaces and best-fit exponential decrease models (solid line) and models with minimum and maximum average inheritance (dashed lines).

the Gobi-Altay. It is composed of three massifs named Ih Bogd, Baga Bogd and Artz Bogd (Fig. 1b). Reverse-left-lateral strike–slip faults are found at the bottom of the three-massif northern flanks. Along Ih Bogd and Baga Bogd massifs, these fault segments belong to the Bogd fault system that ruptured most recently over 270 km long during the 1957 M8.3 Gobi-Altay earthquake. Reverse faulting is also present along Ih Bogd and Baga Bogd southern flanks, but not along Artz Bogd. In most cases, this reverse faulting is associated with thrusting ridges called 'forebergs' (Bayasgalan *et al*., 1999; Carretier *et al*., 2002).

Morphotectonic analysis and age calculations

We studied three sites corresponding to abandoned alluvial fans that are offset by fault movement (Fig. 1b). Fan surfaces show little erosion as suggested by the heavy desert varnish coatings on the top of the exposed boulders. However, the boulder patina is less developed near the ground suggesting wind deflation. On each site, faulted alluvial surfaces have been mapped using 1/35 000 aerial photographs and field survey (Ritz *et al*., 1995; Carretier, 2000; Ritz *et al*., 2003; this study). Displacements have been calculated from topographic profiles generated by kinematic GPS survey (e.g. Ritz *et al*., 2003) except at Noyan Uul where we kept the left-lateral offsets estimated by Ritz *et al*. (1995).

To determine the exposure ages of the alluvial surfaces, we analysed the concentration of *in situ* produced ^{10}Be that accumulates through time in quartz-rich cobbles exposed to cosmic rays (e.g. Brown *et al*., 1991; Lal, 1991) (Table 1). In order to improve the dating, we analysed the ^{10}Be distribution at depth along soil pits dug into the first metres of the surfaces (for sampling strategy see Ritz *et al*., 2003). On one hand, if the ^{10}Be concentrations show the expected exponential decrease, this technique ensures that samples have evolved *in situ* since their emplacement. The distribution along the profile is then a function of the exposure time and of the erosion rate (e.g. Brown *et al*., 1992). On the other hand, this technique allows estimating the average ^{10}Be inheritance of the surface, which accumulates during the exhumation and the transport of the material before the deposit. If not taken into account, inherited ^{10}Be leads to the overestimation of the surface exposure age (e.g. Anderson *et al*., 1996; Repka *et al*., 1997; Hancock *et al*., 1999). Inheritance is defined by the asymptote towards which the exponential curve tends below ~2 m, as below this depth the post-depositional production of ^{10}Be is largely negligible for the time range we are dealing with (Burbank and Anderson, 2001).

Exposure ages were calculated by using the equations and the estimates of the contribution of the nuclear particles proposed by Braucher *et al*. (2003). For each profile, using a least square inversion procedure and testing among a range of inheritance values, we determined the time and the erosion rate corresponding to the best-fit model. For each site we processed the data taking into account the available morphotectonic constraints (multiple cumulated offset of the markers, estimates on the erosion rates, stratigraphy).

Noyan Uul

The studied site is located along the Bogd fault (Fig. 1b), in a zone where each main drainage basin is associated with a sequence of three faulted alluvial fans of different ages (Ritz *et al*., 1995; Carretier *et al*., 1998; Ritz, 2003). The apexes of these surfaces are misaligned with regard to their respective drainage basin outlets due to left-lateral movement with a reverse component along the fault (Fig. 2). Ritz *et al*. (1995) sampled S1 and S2 that are displaced 110 ± 10 and 220 ± 10 m, respectively. If we

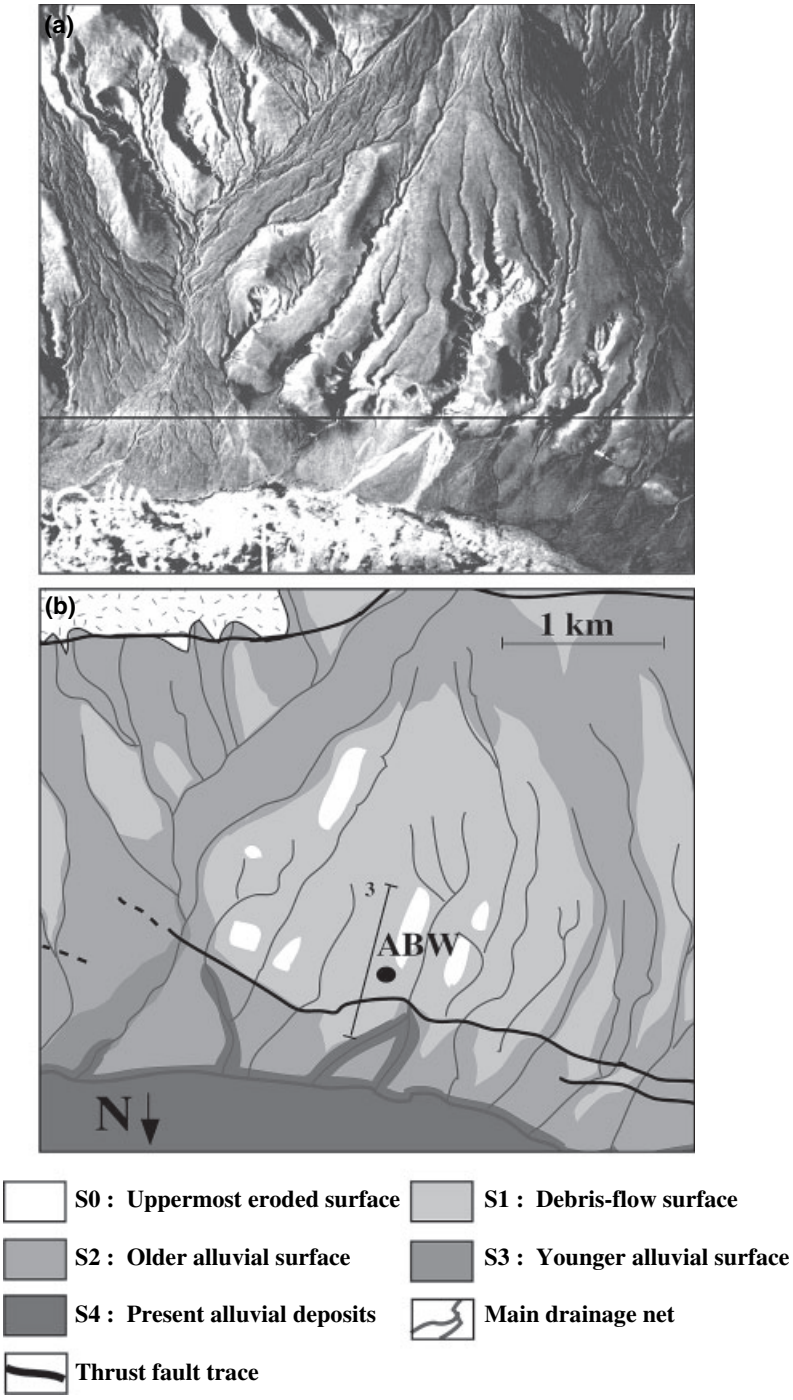

Fig. 6 (a) Aerial photograph of the studied site along the thrust fault to the North of Artz Bogd. (b) Corresponding detailed morphotectonic map with the location of the ^{10}Be sampling site and of the topographic profile (see Fig. 7a).

consider a constant slip rate through time, surface S2 is twice older than S1. The ^{10}Be concentration on surface S2 should be twice that of S1. Instead, Ritz *et al.* (1995) found that there were minor variations of ^{10}Be concentrations between the two surfaces, which suggested that the concentrations are approaching steady-state values. Taking the apparent age calculated for the youngest surface S1, they calculated a maximum horizontal slip rate of 1.2 mm yr^{-1} that was recently re-evaluated to 1.5 ± 0.4 mm yr^{-1} after correction on the production rate (Ritz *et al.*, 2003).

In this study, we re-sampled surface S1 and analysed the ^{10}Be distribution at depth. The best-fit model explaining the distribution of ^{10}Be along the profile gives a ^{10}Be surface concentration of 1.7 ± 0.05 Mat g^{-1} for an average inheritance of 0.20 ± 0.10 Mat g^{-1} (Fig. 3a). To better constrain the erosion rate, we put together S1 surface concentration (given by the model, C1), the difference in surface concentration between S1 and S2 [found by Ritz *et al.* (1995), $\Delta = 0.29 \pm 0.13$ Mat g^{-1}] and the age ratio between the two surfaces ($T_2 = 2T_1$). We obtained a single value of 7 ± 1 m Ma^{-1} (Fig. 3b). This allows us to calculate the age of S1 at 125 ± 28 ka, which in turn gives an age of 250 ± 56 ka for S2. These ages correspond to the end of the marine isotope stages (MIS) 6 and 8 and yield a left-lateral slip rate of 0.95 ± 0.29 mm yr^{-1} along the Bogd fault.

Gurvan Bulag

At the southern foothills of Ih Bogd massif, we studied two stepped alluvial surfaces (IBSA and IBSB) that are affected by the Gurvan Bulag thrust fault (Fig. 1b). These surfaces are found both in the hangingwall and in the footwall, which allows an accurate estimate of their vertical offsets (Fig. 4). The younger surface (IBSB) is vertically displaced by 5.0 ± 0.5 m and the older surface (IBSA) by 16.0 ± 0.5 m (Fig. 5a). The distribution of ^{10}Be concentration at depth in both surfaces shows an exponential decrease (Fig. 5b). We determined average inherited ^{10}Be concentrations of 0.20 ± 0.05 Mat g^{-1} for IBSB and 0.30 ± 0.10 Mat g^{-1} for IBSA. Considering the 2.5 ± 0.5 mMa^{-1} erosion rate estimated by Ritz *et al.* (2003) on an adjacent fan, we calculated the abandonment of IBSB and IBSA surfaces at 22 ± 3 and 128 ± 13 ka, respectively. These ages are consistent with those obtained by Ritz *et al.* (2003) on nearby surfaces and correspond to the end of MIS 2 and 6.

As we do not know when during the seismic cycle IBSA and IBSB surfaces were formed, we bracketed the vertical slip rates with the total offsets and the total offsets minus the mean 1957

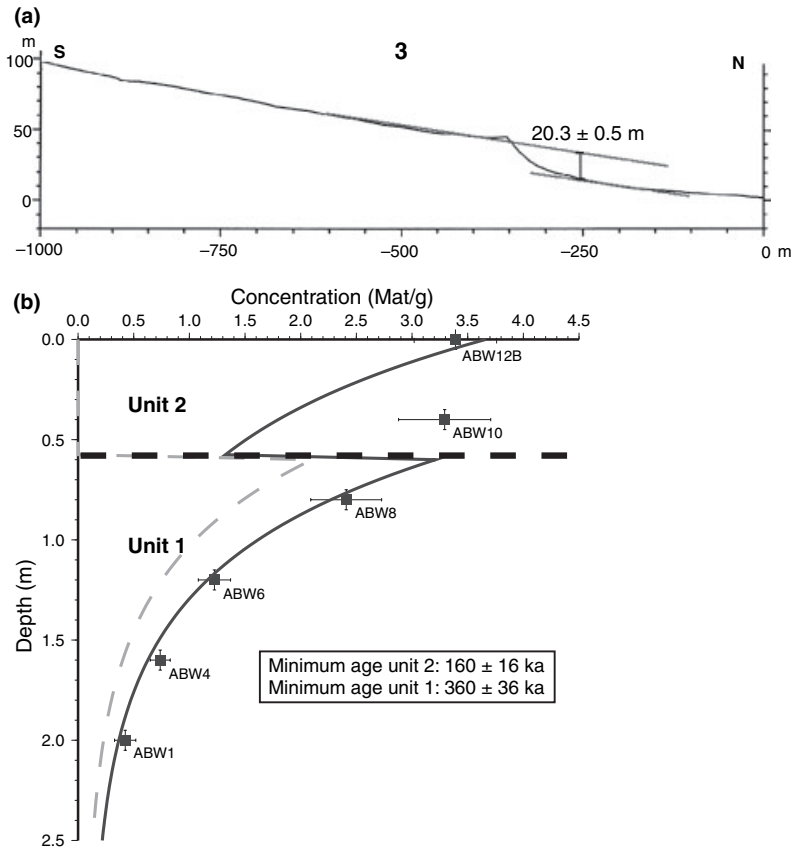

Fig. 7 (a) Topographic profile across the surface and vertical offset at Artz Bogd site. (b) Results of the ^{10}Be analysis. The ^{10}Be distribution in Unit 1 before deposit of Unit 2 (with removal of ~40 cm of Unit 1) is in dashed line, the present distribution is in solid line.

vertical offset. Taking into account the palaeoseismological data (Prentice *et al.*, 2002), we estimated the latter at ~1 m. Dividing the offset values by the ages of IBSB and IBSA surfaces yields upper and lower limits on the vertical slip rates of 0.23 ± 0.05 and 0.19 ± 0.05 mm yr^{-1} for the past ~20 ka, and of 0.13 ± 0.02 and 0.12 ± 0.02 mm yr^{-1} for the past ~125 ka, respectively. These results confirm that the activity along the Gurvan Bulag thrust fault increased during the past ~20 ka, but in a lower proportion than proposed by Ritz *et al.* (2003).

Artz Bogd

The studied site is situated at the western termination of the thrust fault associated with the foreberg on the northern flank of Artz Bogd massif (Fig. 1b). We studied an uplifted alluvial–colluvial surface that is vertically displaced by the thrust fault (Fig. 6). We are not sure whether the surface extending downslope the fault scarp corresponds to the surface that is vertically offset in the hangingwall. The planar hangingwall surface is vertically separated by 20.3 ± 0.5 m with respect to the footwall surface (Fig. 7a).

Distribution of ^{10}Be at depth along a soil pit dug in the hangingwall surface suggests the overlapping of two depositional sequences (Fig. 7b). This is consistent with the stratigraphy observed in the pit, which shows a ~60 cm layer (Unit 2) mainly characterized by debris flow deposits covering another layer (Unit 1) made of smaller debris (S. Carretier, unpublished data).

The distribution of the ^{10}Be concentration at depth within the lower deposits is perfectly explained by a model without inheritance. On the other hand, the concentration of the sample ABW10 in the upper deposits shows an inheritance due to an earlier exposure. A simple interpretation is that sample ABW10 has been remobilized from Unit 1 into Unit 2, and therefore has been exposed twice at different depths. Considering this scenario, the best-fit model for the entire profile takes into account the ^{10}Be concentration of all samples, the removal of a certain thickness of Unit 1 at the time of deposition of Unit 2 and the assumption of no erosional losses. This yields a minimum age of 360 ± 36 and 160 ± 16 ka for Units 1 and 2, respectively. The formation of Unit 1 looks coeval with the global climatic change at the end of MIS 10, while the formation of Unit 2 would be correlated with a minor pulse during the penultimate glacial stage. The incision of the surface by the drainage network due to regressive erosion is clearly posterior to the vertical displacement of the overall deposits, which yields a maximum vertical slip rate of 0.13 ± 0.01 mm yr^{-1} for the last 160 ka.

Conclusions

This study provides further data to previous morphotectonic works within the Gurvan Bogd system. It improves the exposure age estimates of faulted morphological markers and documents tectonic and climatic processes in the area.

As regards the slip-rate estimations along the faults, our data allow re-estimating the Bogd fault left-lateral slip rate at 0.95 ± 0.29 mm yr^{-1} over the past ~250 ka. We confirm that the thrust faults within the Gurvan Bogd system have Upper Pleistocene vertical slip rates comprised between 0.12 ± 0.02 and 0.13 ± 0.02 mm yr^{-1} and that fault activity slightly increased along the Gurvan Bulag thrust fault during the past ~20 ka.

As regards the regional climate history, our ^{10}Be data strengthen the idea of major pulses of aggradation localized in time. The data account for four major alluviations at ~20, 120, 250 and 360 ka, at the terminations of MIS 2, 6, 8 and 10, respectively (Fig. 8). Thus, these pulses would occur at the transition from glacial to interglacial periods, when the global climate becomes warmer and wetter. This predominant climatic control

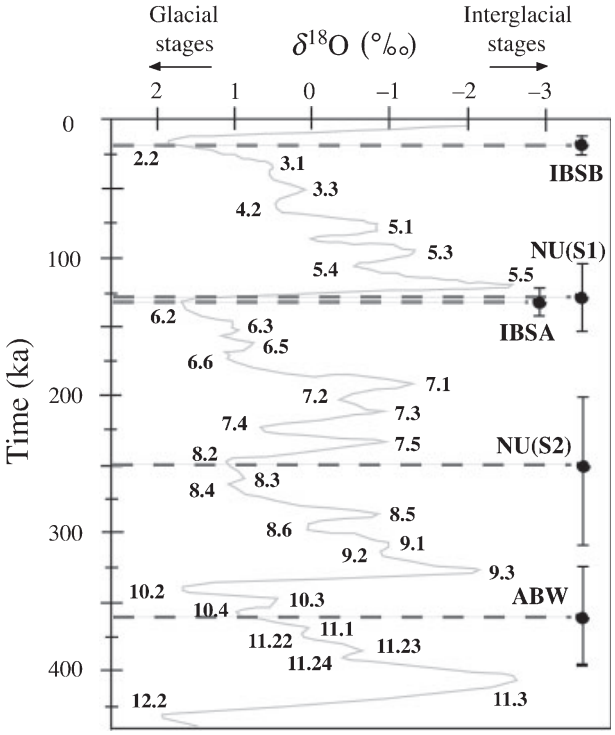

Fig. 8 Correlation between the ^{10}Be ages of the alluvial fans formed within the Gurvan Bogd mountain range and the oxygen isotope curve for Pleistocene and Holocene (Low Latitude Stack, MD900963 + Site 677) modified after Imbrie *et al.* (1984). ^{10}Be age of the Artz Bogd surface (ABW, Unit 1) is a minimum age; error bars for the age of S2 surface at Noyan Uul are larger than the others because this age is indirectly calculated from that of S1.

on the genesis of morphological markers has been also observed in NW China (Pan *et al.*, 2003).

Analysis of the distribution of ^{10}Be concentration at depth within different alluvial surfaces of different ages around Ih Bogd massif shows similar inherited concentrations (0.2–0.3 Mat g^{-1}). This suggests a regular process for the exhumation–transport of the material before its abandonment within alluvial fans. The low sample-to-sample variability in inheritance suggests a stochastic production history. This pattern probably corresponds to the pre-exposure of the material during the transport in the drainage network rather than during its exhumation (see Repka *et al.*, 1997). This also explains the absence of inheritance at Artz Bogd site, where the drainage basins are small (compared to Ih Bogd) involving a rapid transport. If we consider an average burying depth throughout the transport comprised between 0 and 1 m (corresponding to the mean diameter of the largest boulders), the 0.2–0.3 Mat g^{-1} of inherited ^{10}Be account for a pre-exposure time in the drainage network comprised between 5–6 and 30–40 kyr.

Acknowledgements

This study was supported by the Laboratory Dynamique de la Lithosphere-UMR5573 in Montpellier, by the CEREGE, and by the CNRS-INSU PICS Mongolie-Baikal program. We thank James Jackson, Amgalan Bayasgalan, Didier Bourlès and Marc Jolivet for fruitful discussions. We acknowledge D. W. Cunningham and an anonymous referee for their reviews that helped us to improve the original manuscript. We are also thankful to Vivien Iredale and Italia Merano for the correction of the English.

References

Anderson, R.S., Repka, J.L. and Dick, G.S., 1996. Explicit treatment of inheritance in dating depositional surfaces using in situ ^{10}Be and ^{26}Al. *Geology*, **24**, 47–51.

Baljinnyam, I., Bayasgalan, A., Borisov, B.A., Cisternas, A., Dem'yanovich, M.G., Ganbaatar, L., Kochetkov, V.M., Kurushin, R.A., Molnar, P., Philip, H. and Vashchilov, Yu.Ya., 1993. Ruptures of major earthquakes and active deformation in Mongolia and its surroundings. *Geol. Soc. Am. Mem.*, **181**, 62.

Bayasgalan, A., Jackson, J., Ritz, J.F. and Carretier, S., 1999. Field examples of strike–slip terminations in Mongolia, and their tectonic significance. *Tectonics*, **18**, 394–441.

Braucher, R., Brown, E.T., Bourlès, D.L. and Colin, F., 2003. Insitu produced ^{10}Be measurements at great depths: implications for production rates by fast muons. *Earth Planet Sci. Lett.*, **211**, 251–258.

Brook, E.J., Kurz, M.D., Denton, G.H. and Ackert, R.P. Jr, 1993. Chronology of Taylor glacier advances in Arena Valley, Antarctica, using in situ cosmogenic ^{3}He and ^{10}Be. *Quatern. Res.*, **39**, 11–23.

Brown, E.T., Edmond, J.M., Raisbeck, G.M., Yiou F., Kurz, M.D. and Brook, E.J., 1991. Examination of surface exposure ages of Antarctic moraines using in situ produced ^{10}Be et^{26}Al. *Geochim. Cosmochim. Acta*, **55**, 2699–2703.

Brown, E.T., Brook, E.J., Raisbeck, G.M., Yiou F. and Kurz, M.D., 1992. Effective attenuation lengths of cosmic rays producing ^{10}Be and ^{26}Al in quartz: implication for exposure age dating. *Geophys. Res. Lett.*, **19**, 369–372.

Brown, E.T., Bendick, R., Bourlès, D.L., Gaur, V., Molnar, P., Raisbeck, G.M. and Yiou, F., 2002. Slip rates of the Karakorum fault, Ladakh, India, determined using cosmic ray exposure dating of debris flows and moraines. *J. Geophys. Res.*, **107**(B9), 2192, doi:10.1029/2000JB000100.

Burbank, D.W. and Anderson, R.S., 2001. *Tectonic Geomorphology*. Blackwell Science, Malden, USA, p. 274.

Carretier, S., 2000. *Cycle sismique et surrection de la chaîne de Gurvan Bogd (Mongolie). Approche de la géomorphologie quantitative*, PhD thesis, Université de Montpellier 2, p. 324.

Carretier, S., Lucazeau, F. and Ritz, J.F., 1998. Approche numérique des intéractions entre climat, faille active et érosion. *CR Acad. Sci. Paris*, **326**, 391–397.

Carretier, S., Ritz, J.F., Jackson, J. and Bayasgalan, A., 2002. Morphological dating of cumulative reverse fault scarp: examples from the Gurvan Bogd fault system, Mongolia. *Geophys. J. Int.*, **148**, 256–277.

Cunningham, D.W., Windley, B.F., Dorjnamjaa, D., Badamgarov, G. and Saandar, M., 1996. A structural transect across the Mongolian Western Altai: active transpressional mountain building in central Asia. *Tectonics*, **15**, 142–156.

Florensov, N.A. and Solonenko, V.P. (eds), 1965. *The Gobi-Altay Earthquake*. US Department of Commerce, Washington, DC.

Hancock, G.S., Anderson, R.S., Chadwick, O.A. and Finkel, R.C., 1999. Dating fluvial terraces with ^{10}Be and ^{26}Al profiles: application to the Wind River, Wyoming. *Geomorphology* **27**, 41–60.

Hanks, T.C., Ritz, J.F., Kendrick, K.J., Finkel, R.C. and Garvin, C.D., 1997. Uplift rates in a continental interior: faulting offsets of a ~100 ka abandoned fan along the Bogd fault, southern Mongolia. *Proc. Penrose Conf. Tecton Cont. Int.*, 23–28 September, Cedar City, UT.

Imbrie, J., Hays, J.D., Martinson, D.G., McIntyre, A., Mix, A.C., Morley, J.J., Pisias, N.G., Prell, W.L. and Shackleton, N.J., 1984. The orbital theory of Pleistocene climate: support from a revised chronology of the marine d18O record. In: *Milankovitch and Climate* (A.L. Berger, J. Imbrie, J. Hays, G. Kukla and B. Saltzman, eds), pp. 269–305. D. Riedel, Hingham, MA.

Kurushin, R.A., Bayasgalan, A., Ölziybat, M., Enkhtuvshin, B., Molnar, P., Bayarsayhan, C., Hudnut, K.W. and Lin J., 1997. The surface rupture of the 1957 Gobi-Altay, Mongolia, earthquake. *Geol. Soc. Am. Spec. Pap.*, **320**, 143.

Lal, D., 1991. Cosmic ray labeling of erosion surfaces: in situ nuclide production rates and erosion models. *Earth Planet. Sci. Lett.*, **104**, 424–439.

McCalpin, J.P., 1996. *Paleoseismology*. Academic, San Diego, CA, p. 588.

Pan, B., Burbank, D., Wang, Y., Wu, G., Li J. and Guan, Q. 2003. A 900 k. y. record of strath terrace formation during glacial-interglacial transitions in northwest China. *Geology*, **31**, 957–960.

Prentice, C., Kendrick, K., Berryman, K., Bayasgalan, A., Ritz, J.F. and Spencer, J.Q., 2002. Prehistoric ruptures of the Gurvan Bulag fault, Gobi Altay, Mongolia. *J. Geophys. Res.*, **107**, 2321.

Raisbeck, G.M., Yiou, F., Bourlès, D.L., Lestringuez, J. and Deboffe, D. 1987. Measurements of ^{10}Be and ^{26}Al with a Tandetron AMS facility. *Nucl. Instrum. Meth.*, **29**, 22–27.

Repka, J.L., Anderson, R.S. and Finkel, R.C., 1997. Cosmogenic dating of fluvial terraces, Fremont River, Utah. *Earth Planet. Sci. Lett.*, **152**, 59–73.

Ritz, J.F., 2003. *Analyse de la tectonique active en domaine continental: Approche morphotectonique et paléosismologique*. HDR thesis, V1 Université de Montpellier 2, p. 72.

Ritz, J.F., Brown, E.T., Bourlès, D.L., Philip, H., Schlupp, A., Raisbeck, G.M., Yiou, F. and Enkhtuvshin, B., 1995. Slip rates along active faults estimated with cosmic-ray-exposure dates: application to the Bogd fault, Gobi-Altaï, Mongolia. *Geology*, **23**, 1019–1022.

Ritz, J.F., Bourlès, D., Brown, E.T., Carretier, S., Chery, J., Enhtuvushin, B., Galsan, P., Finkel, R.C., Hanks, T.C., Kendrick, K.J., Philip, H., Raisbeck, G., Schlupp, A., Schwartz, D.P. and Yiou, F., 2003. Late Pleistocene to Holocene slip rates for the Gurvan Bulag thrust fault (Gobi-Altay, Mongolia) estimated with ^{10}Be dates. *J. Geophys. Res.*, **108** (B3), 2162, doi: 10.1029/2001JB000553.

Schlupp, A., 1996. *Neotectonique de la Mongolie occidentale. Analyse à partir de données de terrain, sismologiques et satellitaires*. PhD thesis, Université de Strasbourg, p. 172.

Tapponnier, P. and Molnar, P., 1979. Active faulting and Cenozoic tectonics of the Tien Shan, Mongolian and Baykal regions. *J. Geophys. Res.*, **84**, 3425–3459.

Van der Woerd, J., Ryerson, F.J., Tapponnier, P., Gaudemer, Y., Finkel, R., Meriaux, A.S., Caffee, M., Guoguang, Z. and Qunlu, H., 1998. Holocene left-slip rate determined by cosmogenic surface dating on the Xidatan segment of the Kunlun fault (Qinghai, China). *Geology*, **26**, 695–698.

Yeats, R. and Prentice, C., 1996. Introduction to special section: paleoseismology. *J. Geophys. Res.*, **101**, 5847–5853.

Received 9 August 2004; revised version accepted 23 January 2005

